Entropic trap, surface-mediated combing, and assembly of DNA molecules within submicrometer interfacial confinement

Shu-Fu Hsieh and Hsien-Hung Wei*

Department of Chemical Engineering and Center for Micro/Nano Science and Technology, National Cheng Kung University, Tainan 701, Taiwan

(Received 1 August 2008; published 2 February 2009)

In this work, we report an alternative microfluidic approach to studying the motion of single DNA molecules in an electric field. Making use of a closely fitting droplet in a microchannel, DNA molecules can be confined within the submicrometer film beneath the droplet. Several dynamic events at the single-molecule level and self-assembly phenomena at mesoscales are observed. We find that DNA can be trapped and stretched at the entrance to the film due to entropic effects. After escaping the trap, DNA can exhibit cyclic stick-slip motion with a field-dependent mobility owing to interim anchoring to surface surfactants. We also observe that, by incorporation of surface modification effects with plasma oxidation, DNA can be combed onto the channel surface at sufficiently high fields. In this case, upon removing the field, as-stretched DNA molecules can aggregate into larger clusters or self-organize into mesoscale bundles aligned in the direction of the previously applied field. The physics underlying these phenomena is discussed in detail.

DOI: 10.1103/PhysRevE.79.021901 PACS number(s): 87.15.hg, 87.15.hp, 87.15.nr

I. INTRODUCTION

Thanks to the recent advance in nano- and microtechnology, it is now possible to realize programmable manipulation of submicron objects on an integrated, miniaturized platform. Among many efforts toward this end, manipulation of DNA molecules has been drawing particular attention, because not only can it provide a fundamental understanding of the rheological behavior of polymers [1,2], but it can also be applied to extract genetic information [3]. A judicious control of the motion of DNA in structured nanochannels further provides an alternative for sizing DNA on a gel-free basis [4,5]. Because a DNA molecule comprises nucleotides that permit physical and chemical binding to other substances, it can also serve as a molecular template, through appropriate tailoring of its conformation, for realizing self-assembly of nanostructures or construction of functionalized building blocks [6]. However, as a DNA molecule is typically a long polymer chain in the size of 10–1000 kilo base pairs (kbp) and naturally appears in the random coil form, it must be first unraveled by overcoming the elastic recoil of the chain with a sufficiently large stretching force. More precisely, an applied stretching force must be exerted in such a way that it produces large enough velocity or force gradients over a DNA molecule to render a rapid extension of the chain within a time scale τ_{ex} no greater than its characteristic relaxation time τ. That is, the Deborah number $De=\tau/\tau_{ex}$, the ratio between these two time scales, must be of the order of unity or larger. In addition, when system length scales are down to nano- or submicrometer levels, DNA must inevitably change its conformation to minimize its free energy for compensating the entropy loss due to confinement [4], which provides an added advantage for controlling the manipulation.

In view of the above, it is therefore most desirable to manipulate DNA with nano- and microfabrication techniques. Many strategies have been developed along this line. By tethering a DNA molecule on a surface or attaching it to a bead, one can stretch it by pulling at its free end with hydrodynamic flows [7], electric fields [8], and optical or magnetic tweezers [9,10]. One can stretch a freely suspended DNA molecule using hydrodynamic focusing [11] or force and field gradients in nonuniform channel geometries such as cross slots [12,13] and converging channels [3,14]. Other techniques have also been shown to be effective to stretch DNA molecules, including hooking of DNA over obstacles [15], electrophoretically driven reptation in gel matrices or nanopillar arrays [16], redirection of DNA in nanoslits [17], and combing of DNA molecules onto a surface by a moving interface [18,19]. The up-to-date developments for linearization of DNA can be found in the recent review [20].

In this paper, we develop an alternative microfluidic approach to studying the motion of confined DNA molecules in an electric field. Here we invoke a submicrometer film created by a closely fitting microdroplet and utilize this interfacial confinement for stretching DNA beneath the droplet. Compared to existing methods, this platform has the following features. First, the design constitutes only regular 100-μm-sized microchannels. Hence, the fabrication is simple; neither sophisticated geometries nor fine structures are needed. Second, since the electric current must be maintained constant in any conductive passages and the droplet is virtually insulated, the electric field in the film can be augmented with a much greater intensity due to the narrowing of the available cross sectional area for an applied field. This feature not only facilitates stretching DNA [21], but also reduces the voltage needed for driving DNA molecules, which eliminates potential bubble formation or Joule heating problems. Third, because of the large surface-to-volume ratio, the submicrometer film can also render appreciable interactions between confined DNA molecules and the channel surface. Since such interactions can be regulated by modification of the channel surface, the effects can further mediate the DNA motion within the film. With these features, as we will dem-

*Corresponding author. hhwei@mail.ncku.edu.tw

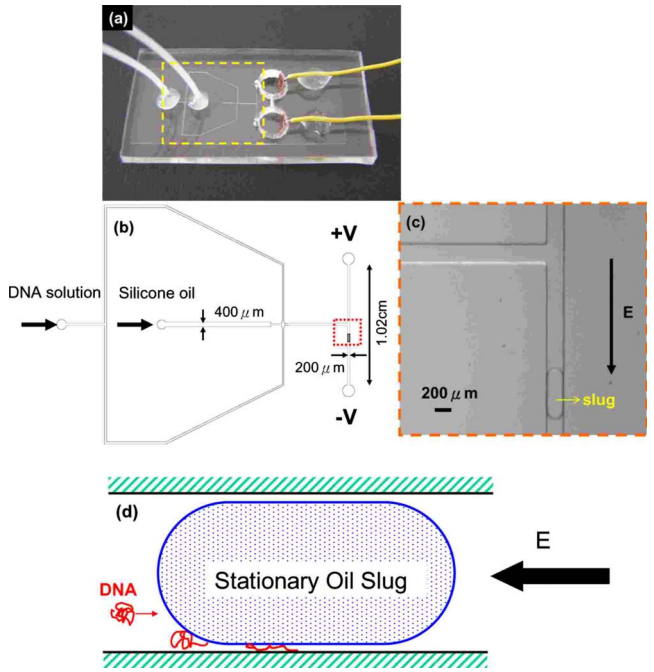

FIG. 1. (Color online) Experimental setup for stretching DNA beneath a microdroplet with electric fields. (a) Microfluidic device. (b) Blow-up view of the highlighted area in (a). A closely fitting slug is generated in the channel system in the left and then redirected to the designated section in the right (highlighted in red). (c) Blow-up view of the slug section. (d) A confined DNA molecule can deform and stretch due to the nonuniform electric field beneath the cap of the slug during its entry to the film.

onstrate shortly, not only can a variety of single-molecule events of DNA be realized, but also additional self-assembly phenomena can emerge.

II. EXPERIMENTAL SECTION

Figure 1 shows the setup of our microfluidic system. The system basically consists of two parts: one for producing a closely fitting microdroplet, and the other for stretching DNA beneath the droplet. The entire channel system is made by polydimethylsiloxane (PDMS) and fabricated with standard photolithography techniques. After being sealed by a glass substrate and assembled with tubing, the entire device is treated by plasma exposure for 1–3 h, where the plasma is operated at radio frequency of 8–12 MHz, power of 29.6 W, and vacuum of 0.1–0.3 torr.

The DNA solution was made by preparing T4-DNA (165.6 kbp, Nippon Gene) of 3 μg/ml in a pH=8 buffer solution containing 10 mM Tris-HCl solution, 10 mM NaCl, and 2 mM ethylene diamine tetra-acetic acid (EDTA) with the addition of 4% 2-mercaptoethanol. The T4-DNA molecules were labeled with YOYO-1 fluorescence dye every five base pairs. We further added 2.2% Tween 20 nonionic surfactant (molecular weight 1228, Sigma) to the solution for preventing the droplet from being in contact with the channel wall. The conductivity of the solution is about 2000 μS/cm and the corresponding thickness of the electric double layer is 2 nm.

The generation of the droplet was carried out in a cross-slot microchannel according to the following procedures. We first filled the channel with the solution, followed by injecting silicone oil (50 cP, Fluka) at 100 μl/h in the horizontal portion of the channel. After pumping the solution and silicone oil at the respective flow rates of 43 and 100 μl/h, a closely fitting oil droplet of 550 μm in length was created. This droplet displaced the solution and in turn created a submicrometer film between the droplet and the channel surface. To estimate the film thickness, we employ negatively charged latex particles of various sizes and drive them into the film with electric fields. Since the film now acts like a sieving slit that allows smaller particles to enter but blocks larger ones, we can estimate the film thickness as 0.92 μm by observing the behavior of these particles at the entrance to the film. The microdroplet was then redirected to the designated channel (of 200 μm in width and 120 μm in height) for observing the DNA motion under electric fields. The motion of DNA was set by dc voltage in the range 7–70 V with the corresponding electric field 30–300 V/cm within the film. The dynamics of DNA molecules within the film were visualized using a fluorescence microscope (Nikon 2000S) with a 100× oil immersion objective lens, and recorded by an intensified charge-coupled device camera (Cool SNAP HQ^2, Roger Scientific).

III. ENTROPIC TRAP BY INTERFACIAL CONSTRICTION

Upon the application of an electric field, DNA molecules migrate toward the positive pole due mostly to electrophoresis because of the negative charge on the backbone, while the droplet still remains stationary (unless the applied voltage is higher than 90 V). Since DNA remains coiled in the bulk and has the radius of gyration $R_g=0.97\pm0.16$ μm (taken from images), it tends to be blocked by constriction in the meniscus region and hence can be trapped entropically at the entrance to the film.

Figure 2 shows sequential images at the entrance of the front meniscus beneath which a few DNA molecules can escape the trap by just gaining enough energy at the critical field of 28.5 V/cm. It clearly shows that these DNA molecules are temporarily trapped within the constriction followed by conformation changes before extending out into the film [Figs. 2(a)–2(c)]. After crossing the constriction, they can travel through the film in a stick-slip manner [Figs. 2(d)–2(f)], which will be discussed later in Sec. IV. Although an entropic trap has been previously reported using a nanochannel with alternating constrictions [4], the phenomenon observed here is demonstrated using an interfacial constriction in a straight channel geometry. Note here that, while DNA molecules can be jammed by the constriction, they can still move along the cap and enter freely the lateral gap regions, as these regions are 20 μm wide and large enough to allow micrometer-sized DNA globules to move in without blockage.

Similar to the kinetic model sketched in Ref. [4], the observed entropic trapping can be understood in terms of the free energy landscape in the constriction region. This free energy is given by

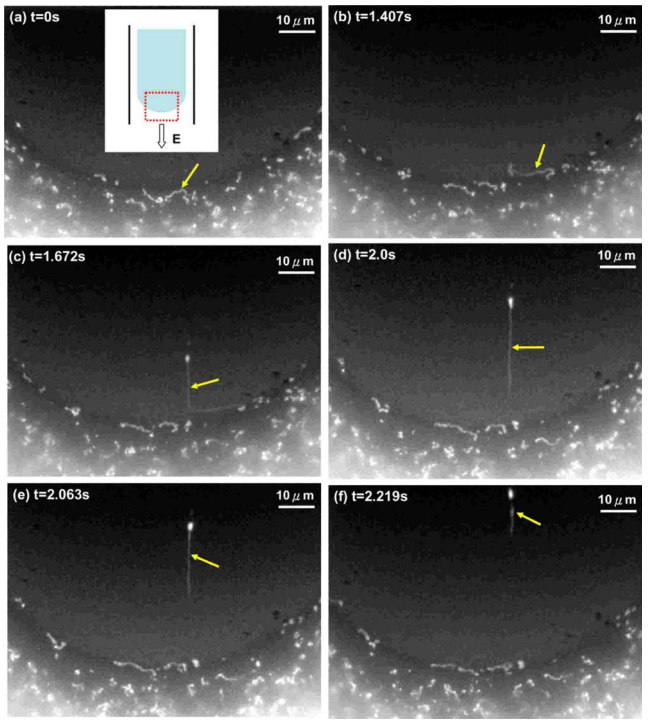

FIG. 2. (Color online) Snapshots of the DNA motion when crossing the constriction beneath the front cap of the slug. The images are taken at the critical field $E=28.5$ V/cm at which a DNA molecule just gains enough energy to overcome the entropic barrier set up by the constriction. A DNA molecule is first trapped at the entrance (a) and (b). It undergoes conformation change and stretch during translocation (c) and (d), and then escapes the trap (e) and (f).

$$\Delta F = \Delta F_{\text{entropic}} + \Delta F_{\text{electric}}, \tag{1}$$

which involves a competition between the increase in the conformational entropic energy $\Delta F_{\text{entropic}}$ and the decrease in the driving electric potential $\Delta F_{\text{electric}}$. As a confined DNA molecule tends to extend itself and looks like a "stem flower ," the associated free energy due to this conformation change is

$$\Delta F_{\text{entropic}} = -(2R_g/h)^{5/3} k_B T + (x/\ell_p) k_B T > 0, \tag{2}$$

where h is the film thickness, ℓ_p is the persistence length ($\sim$100 nm) of the DNA, $2R_g$ is the size of the coiled flower, x ($\gg \ell_p$) is the length of the elongated stem, and $k_B T$ is the thermal energy. The first term is the entropic increase for the flower when it is squeezed into the film by osmotic forces from the DNA-rich bulk toward the DNA-scarce film [22]. The second term is the entropic loss for the stem due to the extension of the chain.

On the other hand, the application of an electric field E provides energy to compensate the entropic loss $\Delta F_{\text{entropic}}$ by stretching and sucking the DNA into the film:

$$\Delta F_{\text{electric}} = -\alpha \eta \mu E x^2 < 0. \tag{3}$$

This energy can be thought of as the work done by a pulling force $f \sim \eta \mu E x$ on the chain, where η is the viscosity of the solution, μ the mobility of the DNA, and α a dimensionless geometrical prefactor.

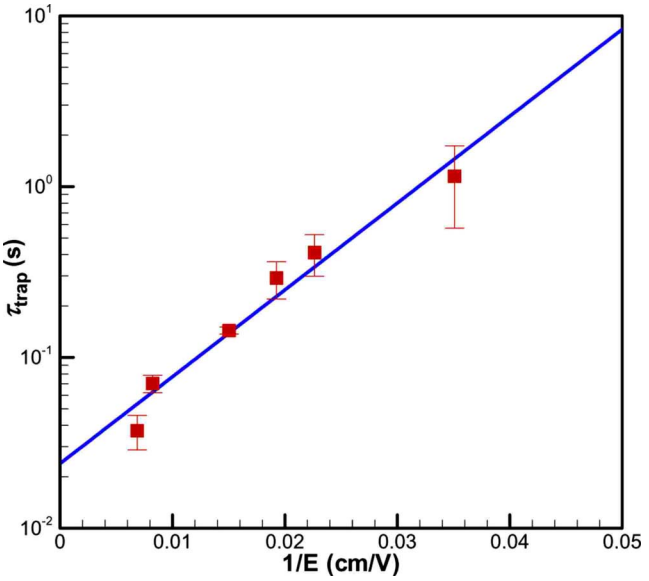

FIG. 3. (Color online) Arrhenius plot of the measured trapping time (symbols) against the inverse applied field within the film. The solid line is the best fit with slope of 117.1 V/cm.

Combining Eqs. (2) and (3), the height of the free energy landscape, the least energy required to activate a DNA molecule to escape from the trap, is

$$\Delta F_{\text{max}}/k_B T = -(2R_g/h)^{5/3} + (E_0/E), \tag{4}$$

with $E_0 = (k_B T/\ell_p)/(4\alpha\eta\mu\ell_p)$ representing the characteristic field for the activation. At weak fields, the barrier is infinitely high and hence DNA is completely blocked by the constriction, while it can readily enter the film at sufficiently high fields. Thereby, there must exist a threshold field at which a DNA molecule just overcomes the entropic barrier to cross the constriction:

$$E_{\text{threshold}} = (h/2R_g)^{5/3} E_0. \tag{5}$$

With the activation energy (4), we can obtain the trapping time with the aid of the Arrhenius law:

$$\tau_{\text{trap}} = \tau_0 \exp(\Delta F_{\text{max}}/k_B T) = \tau_{\text{contact}} \exp(E_0/E). \tag{6}$$

Here $\tau_{\text{contact}} = \tau_0 \exp(-(2R_g/h)^{5/3}) = \tau_0 \exp(-E_0/E_{\text{threshold}})$ is the contact time, whose inverse measures the frequency of a coiled DNA in touch with the constriction; the larger the coil, the more monomers can be exposed to the constriction and hence there is a greater probability per unit time to overcome the barrier [2]. Figure 3 is an Arrhenius plot for the measured trapping time of DNA against $1/E$, and clearly shows the exponential relationship predicted by the present model. In addition, with the fitted slope $E_0 = 117.1$ V/cm, we obtain the threshold field $E_{\text{threshold}} = 33.8$ V/cm, which is in good agreement with the measured value 28.5 V/cm.

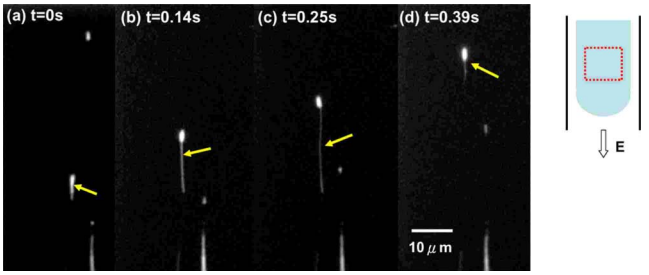

FIG. 4. (Color online) Sequential images of stick-slip DNA motion within the film at $E=28.5$ V/cm. An elongated DNA chain exhibits cyclic stretch and recoil in its motion, suggesting that part of the chain is attached to and then detached from the surface during the journey.

IV. CYCLIC STICK-SLIP MOTION DUE TO INTERIM ANCHORING WITH SURFACE SURFACTANTS

After escaping the trap by overcoming the entropic barrier, a DNA molecule can readily enter the film with a steeper electric potential gradient. However, it does not fully relax back to a coil. As observed in Fig. 4, DNA seems to "stick" and "slip" over the surface in a cyclic stretching-recoiling manner. On some occasions, it can even be stuck completely on the surface.

The observed stick-slip phenomenon is likely attributable to occasional anchoring of an elongated DNA chain to the surfactant sea on the surface. As shown in Fig. 5, because the surface is hydrophilic owing to plasma oxidation, surfactant molecules tend to reorient themselves with their hydrophilic heads toward the surface while leaving their hydrophobic tails exposed to the bulk, creating a surfactant monolayer brush of about 10 nm in thickness on the surface. As an unraveled DNA molecule can also expose its less hydrophilic ends [23], it is more likely to be anchored by the hydrophobic brush of surface surfactants. With this anchoring, DNA can therefore be tethered at the surface, making itself more extendable under the pulling action of the electric field. Indeed, this anchoring is borne out by the evidence that more DNA molecules can be combed on the substrate with longer plasma exposure, which will be shown later in Sec. V. In contrast to Ref. [5], in which DNA can exhibit conformation changes in nanochannels due to surface roughness effects, we find, with the aid of atomic force microscopy (not shown), that surface roughness cannot be responsible for the observed phenomenon because the variations of the roughness are of nanometer size and much smaller than the film thickness. The roughness caused by the surfactant brush is on the order of 10 nm and hence the effects are again insignificant.

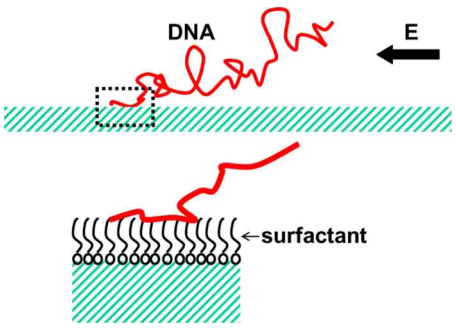

FIG. 5. (Color online) Schematic illustration of how a DNA molecule is anchored by a surfactant brush on the surface.

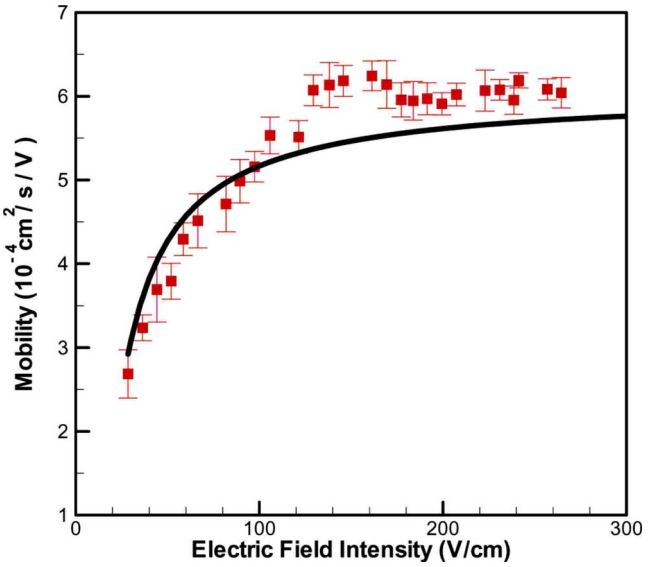

FIG. 6. (Color online) Mobility of T4-DNA (165.5 kbp) within the film as a function of applied field. Red symbols are the measured data. Solid line is the fitted curve using Eq. (7).

Such anchoring, however, is not always strong enough to keep an elongating DNA bound to the surface, as the stretching electric force can also pull the DNA and cause it to detach from the surface. If the anchoring lifetime is long enough to allow a DNA molecule to be stretched further, this linearized DNA will become more susceptible to being combed onto the surface. Otherwise, part of the DNA chain will be temporarily attached to the surface before being pulled away by the electric field. In this case, an elongating DNA molecule, because of its gradually increasing tension, will eventually be detached from the surface, followed by immediate recoil from its detached tail toward the free-moving head. As the DNA now can repeatedly undergo attaching, stretching, detaching, and recoiling during its journey, its motion looks as if it were sliding and hopping over the surface, leading to the cyclic stick-slip phenomenon observed in Fig. 5.

The observed stick-slip DNA motion somewhat resembles the surface electrophoresis phenomenon reported previously [24]. As shown in Fig. 6, the DNA mobility grows linearly with the field at low fields, but reaches a plateau at high fields. In the low-field regime, because the DNA speed is slow, the anchoring time is long, making DNA more inclined to be retarded by the surface. At sufficiently high fields, DNA can move so fast that it can travel freely without being in contact with the surface. There seems to be a small bump in the measured mobility data at $E\sim 150$ V/cm, after which the mobility is nearly constant. This could be attributed to local surfactant buildup (depletion) on the front (rear) part of a DNA molecule when it travels in a surfactant-rich solution

(in which the surfactant concentration is much higher than the critical micelle concentration). The effect could create a small osmotic pressure difference across the DNA molecule and hence slightly speed up or slow down its motion.

To quantify the mobility behavior shown in Fig. 6, we follow Ref. [24] to write the translational mobility μ_{trans} in the simple form

$$\mu_{\text{trans}} = \mu_{\infty}(1 - E_s/E), \tag{7}$$

with μ_{∞} being the mobility of a free DNA molecule when the applied field E is sufficiently high. Here, E_s ($<E$) is the least field required to drive DNA by overcoming the surface drag, which depends on the fraction of the DNA chain attached onto the surface and on the friction coefficient between the chain and the surface [24]. It is also clear that E must be higher than $E_{\text{threshold}}$, which is the prerequisite for DNA to enter the film. Fitting the data with Eq. (7), we find $\mu_{\infty} = (6.06 \pm 0.098) \times 10^{-4}$ cm^2/s V and $E_s = 14.75$ V/cm. Because DNA spends the trapping time τ_{trap} at the entrance and the translation time $\tau_{\text{trans}} = L/(\mu_{\text{trans}}E)$ crossing the film of length L, it takes time $\tau = \tau_{\text{trap}} + \tau_{\text{trans}}$ to complete the entire trip. As the mobility is inversely proportional to the associated time scale, the apparent mobility reads

$$\mu_{\text{app}} = \frac{\mu_{\text{trans}}\tau_{\text{trans}}}{\tau_{\text{trap}} + \tau_{\text{trans}}} = \frac{\mu_{\text{trans}}}{1 + \mu_{\text{trans}}E\tau_{\text{trap}}/L}. \tag{8}$$

As a result, μ_{app} is controlled by the process with the longer time scale. That is, in the "translation" mode $\tau_{\text{trans}} > \tau_{\text{trap}}$, $\mu_{\text{app}} = \mu_{\text{trans}}$; otherwise, $\mu_{\text{app}} \approx \mu_{\text{trap}} \equiv (L/E)/\tau_{\text{trap}}$ in the "trapping" mode $\tau_{\text{trans}} < \tau_{\text{trap}}$. As μ_{app} clearly depends on the size of the DNA, Eq. (8) might suggest potential DNA separation with the combined effects of entropic trapping and surface electrophoresis. A successful separation might be better realized using a series of microdroplets in which the mobility difference between different DNA molecules can become more apparent by alternate switching between the trapping and translation modes.

V. MOLECULAR COMBING AND SELF-ASSEMBLY OF STRETCHED DNA MOLECULES

In the previous section, we have demonstrated that an elongated DNA molecule can be temporarily anchored by the surfactant brush on the surface due to its hydrophobic affinity to the likewise hydrocarbon tails of these surfactants, leading to the observed stick-slip phenomenon. As this hooking effect is created by the absorbed surfactants on the surface, we increase the adsorption of the surfactant on the surface by increasing the hydrophilicity of the surface with 3 h exposure to plasma oxidation. By doing so, DNA will become more susceptible to being tethered by denser surface surfactants, hence making itself more stretchable by an electric field.

As evidenced in Fig. 7(a), a DNA molecule can be extended to as much as 20–30 μm in length, which is about 50% of its contour length 56 μm (=0.34 nm/bp × 165.6 kbp) [25]. In addition, more DNA molecules are combed onto the surfactant-coated surface.

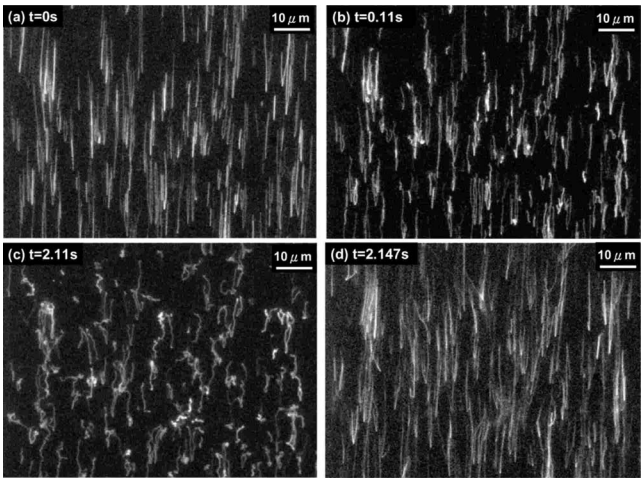

FIG. 7. Reversible molecular combing of DNA assisted by more surfactants absorbed on the surface after 3 h plasma exposure. (a) Initially, DNA molecules are stretched and combed under an electric field $E = 145.7$ V/cm. (b) and (c) depict the relaxation of these DNA molecules after removing the field. (d) The combing immediately recovers when the field is rebooted.

The phenomenon becomes even more apparent at large fields, because stretching of DNA can be promoted by large fields and more DNA molecules can be fed into the film at higher supply rates. These DNA molecules, however, are not bound to the surface indefinitely, as they can still undergo chain relaxation [Fig. 7(b)] when the field is removed. As shown in Figs. 7(c) and 7(d), the combing immediately recovers at the moment when the field is rebooted during the relaxation. The observed relaxation process takes 2–6 s, which is relatively long compared to the typical relaxation time of DNA in micrometer-sized confinement [26]. This finding suggests that a stretched DNA molecule could be entangled with surface surfactants, which leads to a decrease in its chain mobility and hence is responsible for the long relaxation observed in the experiment.

In addition, we observe another phenomenon beyond the usual chain relaxation. As shown in Fig. 8, after removing the field, recoiling DNA molecules can flocculate among themselves. The flocculation appears long range, as these DNA molecules can aggregate into a larger cluster at a distance of 20 μm. The time scale for such a self-aggregation process is about 20 s and hence much longer than the typical DNA relaxation time, suggesting that additional effects must be at play.

A plausible cause for the observed DNA flocculation might be osmotic attraction between localized DNA aggregates. Set up by a cloud of stretched DNA molecules on the surface, these aggregates form due to short-range van der Waals attraction between the DNA molecules. As such aggregates contain many more DNA molecules than the bulk (of concentration far below the overlap concentration $c^* \sim 300$ μg/ml [27]), they behave like swollen globules with buildup of osmotic pressure therein. Accordingly, an aggregate of size R containing monomers of number n has an osmotic pressure $\Pi \sim k_B T n/R^3$. Taking into account excluded volume effects, we find, with the aid of Flory's scaling R

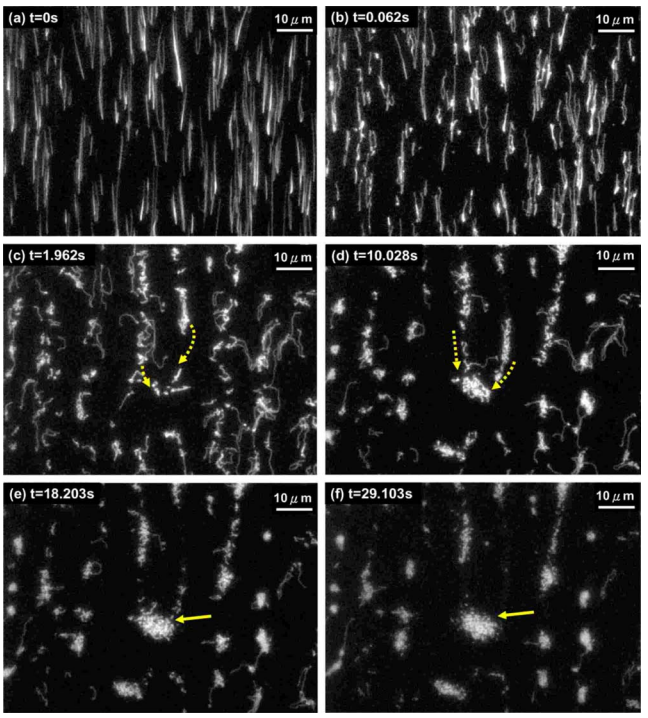

FIG. 8. (Color online) Long-range flocculation of stretched DNA molecules after field $E=223.0$ V/cm is turned off at $t \sim 0.06$ s. Small DNA aggregates self-migrate [along the paths in (c) and (d)] into a larger cluster [indicated by arrows in (e) and (f)].

$\propto n^{3/5}$, that this pressure varies as $1/R^{4/3}$ [22]. Hence, a larger aggregate actually acts like a lower-pressure "sink," tending to drain smaller aggregates around it. As a result, small aggregates will coalesce because of their size differences and larger clusters will continue to grow by attracting smaller ones, giving rise to collective flocculation of DNA molecules. According to the Kedem-Katchalsky law [28], the sink induced by a larger aggregate creates an inward osmotic flow of velocity $U_s \sim L_p \Pi$ around its periphery, where L_p measures the hydraulic permittivity of the water flow. For small aggregates at a distance r away from larger ones, the former will drift toward the latter at a speed of $U \sim U_s(R/r)$ due to the inward osmotic flow (here the flow can be thought of as nearly two dimensional because it occurs on the surface). As such an osmotic suction decays at the rate of r^{-1}, DNA molecules can be gathered remotely, thereby leading to the long-range flocculation observed in Fig. 8.

We also find that the combed DNA molecules at large fields can even develop into bundles after the field is removed, as shown in Fig. 9. As these bundles appear aligned with the previously applied field direction, this suggests that stretched DNA molecules can still maintain their extensions during aggregation. In other words, the relaxation time of these DNA molecules becomes prohibitively long (due to much stronger surface binding) compared to the time scale associated with aggregation between the chains (due to much denser combing).

The observed DNA bundles can be attributed to the combined effects of surfactant-assisted combing, short-range cross linking, and long-range osmotic attraction of stretched DNA molecules. When the anchoring effects are enhanced

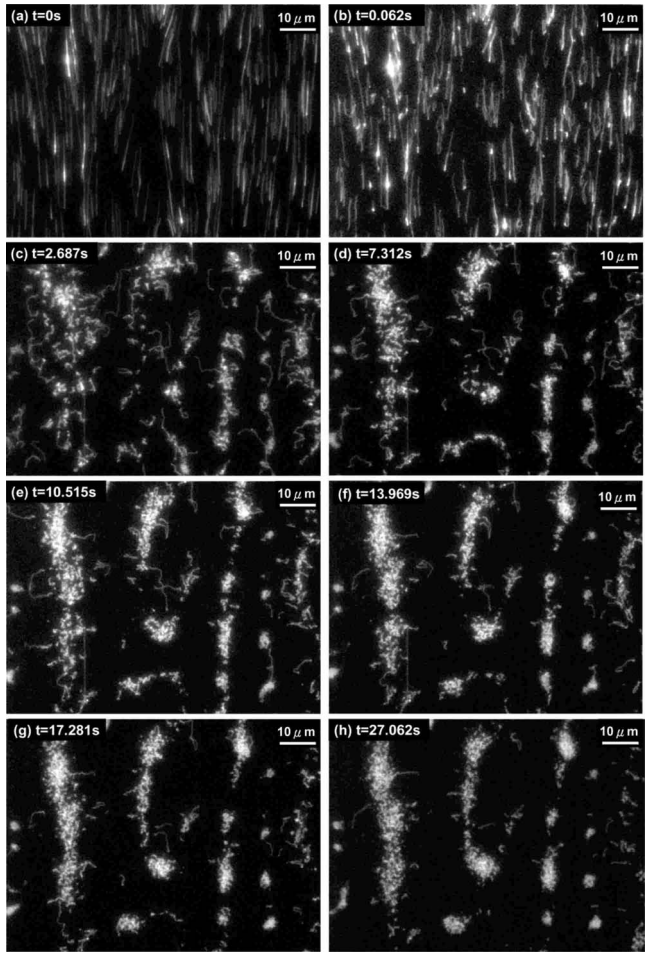

FIG. 9. Formation of DNA bundles. Compared to Fig. 8, the applied field $E=256.9$ V/cm now is higher and more DNA molecules are combed onto the surface. After removing the field at $t \sim 0.06$ s, the combed DNA molecules can self-organize into bundles due to cross links between the elongated chains.

by increasing the surfactant brush density on the surface, DNA can exhibit a longer extension under the pulling action by the electric field, and hence has stronger binding to the surface with surface surfactants. Now, as more DNA molecules can be fed into the film and combed onto the surface at high fields, much denser combing of DNA can result. After removing the field, while these much extended DNA molecules relax gradually, they can still undergo transverse fluctuations along the chains during relaxation. Since such fluctuations can increase the contact between nearby, slowly relaxing DNA chains, the effects will lead to attraction between the chains due to short-range van der Waals forces. Such interchain attraction can be thought of as the interactions between two parallel rods, and the associated van der Waals force can be roughly estimated as $CLa^{-2}r^{-6}$, where C is the coefficient of the pair potential (of $\sim 10^{-77}$ J m^6), L (~ 20 μm) the chain length, a (~ 2 nm) the diameter of DNA, and r the separation between the chains [29]. For the nanometer-sized interchain separation, the estimated attraction force can be as large as piconewtons. Because DNA molecules now become greatly extended and bound by the surface surfactants, they will take a long time to relax. Also,

because these DNA chains are combed on the surface in a rather dense manner, they will cross link laterally through the van der Waals attraction and hence become entangled with each other. Obviously, such self-entanglement is not spatially uniform and at some point must be counterbalanced by electrostatic repulsion or self-avoiding effects between the chains. Consequently, these entangled DNA molecules will sooner or later turn into aggregates of different sizes. As these aggregates can continue to grow into larger islands due to the long-range osmotic attraction mentioned earlier, they eventually clump into the DNA bundles observed in Fig. 9.

As dense combing of DNA molecules is the prerequisite for the observed self-organization phenomena, the confinement effects created by the submicrometer film and the anchoring effects due to surface surfactants furnish the ingredients needed for the combing. Also, because the dispersion behavior of the combed DNA molecules strongly depends on their interactions with surface surfactants, the question of whether these DNA molecules can form a distinct phase with aggregates at large seems to resemble spinodal decomposition or coalescence of microdroplets in the context of the classical phase transition phenomena of binary mixtures [30]. The observed DNA bundles also seem somewhat analogous to self-assembled or phase-segregated liquid crystal molecules [31] in the sense that the phenomenon is a result of cross links between stretched DNA molecules, similar to the formation of anisotropic crystal structures driven by external fields. Detailed accounts of these phenomena require more thorough studies on how confined DNA molecules interact with surface surfactants with and without electric fields.

VI. CONCLUDING REMARKS

In this work, we employ a submicrometer film created by a closely fitting microdroplet and utilize this film to study the motion of confined DNA under the actions of an electric field. Several phenomena, such as entropic trapping, stretching, and escape of DNA, can be realized using this approach. This is a demonstration of single-molecule dynamics using interfacial confinement in a straight channel geometry. We also find that a confined DNA molecule can be dragged by surface surfactants and exhibit stick-slip behavior with a field-dependent mobility. In addition, with surfactant anchoring enhanced by surface modification effects, DNA molecules can not only be combed onto the surface, but can also self-aggregate into larger clusters after the field is removed. In the latter scenario, as-stretched DNA molecules can form mesoscale bundles due to crosslinks between themselves. This report unveils these unusual self-assembly phenomena of confined DNA molecules.

In conclusion, the use of a readily prepared microdroplet in creating confinement effects provides a relatively simple approach to trapping or stretching DNA molecules. As the motion of confined DNA can be further mediated by the interactions with the channel surface, this platform also offers the advantages of molecular combing and self-assembly of DNA.

ACKNOWLEDGMENTS

This work was supported by the National Science Council of Taiwan under Grants No. NSC 96-2221-E-006-055 and No. NSC 97-2628-E-006-001-MY3.

[1] E. S. G. Shaqfeh, J. Non-Newtonian Fluid Mech. **130**, 1 (2005).
[2] G. W. Slater, Y. Gratton, M. Kenward, L. McCormick, and F. Tessier, Soft Mater. **2**, 155 (2004).
[3] E. Y. Chan, N. M. Goncalves, R. A. Haeusler, A. J. Hatch, J. W. Larson, A. M. Maletta, G. R. Yantz, E. D. Carstea, M. Fuchs, G. G. Wong, S. R. Gullans, and R. Gilmanshin, Genome Res. **14**, 1137 (2004).
[4] J. Han, S. W. Turner, and H. G. Craighead, Phys. Rev. Lett. **83**, 1688 (1999).
[5] G. B. Salieb-Beugelaar, J. Teapal, J. V. Nieuwkasteele, D. Wijnperle, J. O. Tegenfeldt, F. Lisdat, A. ven den Berg, and J. C. T. Eijkel, Nano Lett. **8**, 1785 (2008).
[6] H. Yan, S. H. Park, G. Finkelstein, J. H. Reif, and T. H. LaBean, Science **301**, 1882 (2003).
[7] T. T. Perkins, D. E. Smith, R. G. Larson, and S. Chu, Science **268**, 83 (1995).
[8] S. Ferree and H. W. Blanch, Biophys. J. **85**, 2539 (2003).
[9] S. B. Smith, Y. Cui, and C. Bustamante, Science **271**, 795 (1996).
[10] T. R. Strick, J. F. Allemand, D. Bensimon, A. Bensimon, and V. Croquette, Science **271**, 1835 (1996).
[11] P. K. Wong, Y. K. Lee, and C. M. Ho, J. Fluid Mech. **497**, 55 (2003).
[12] T. T. Perkins, D. E. Smith, and S. Chu, Science **276**, 2016 (1997).
[13] Y. J. Juang, S. Wang, X. Hu, and L. J. Lee, Phys. Rev. Lett. **93**, 268105 (2004).
[14] J. W. Larson, G. R. Yantz, Q. Zhong, R. Charnas, C. M. D'Antoni, M. V. Gallo, K. A. Gillis, L. A. Neely, K. M. Phillips, G. G. Wong, S. R. Gullans, and R. Gilmanshin, Lab Chip **6**, 1187 (2006).
[15] O. B. Bakajin, T. A. J. Duke, C. F. Chou, S. S. Chan, R. H. Austin, and E. C. Cox, Phys. Rev. Lett. **80**, 2737 (1998).
[16] W. D. Volkmuth and R. H. Austin, Nature (London) **358**, 600 (1992).
[17] K. Jo, D. M. Dhingra, T. Odijk, J. J. de Pablo, M. D. Graham, R. Runnheim, D. Forrest, and D. C. Schwartz, Proc. Natl. Acad. Sci. U.S.A. **104**, 2673 (2007).
[18] A. Bensimon, A. Simon, A. Chiffaudel, V. Croquette, F. Heslot, and D. Bensimon, Science **265**, 2096 (1994).
[19] C. A. P. Petit and J. D. Carbeck, Nano Lett. **3**, 1141 (2003).
[20] N. Douville, D. Huh, and S. Takayama, Anal. Bioanal. Chem. **391**, 2395 (2008).
[21] S.-F. Hsieh, C.-P. Chang, Y.-J. Juang, and H.-H. Wei, Appl. Phys. Lett. **93**, 084103 (2008).
[22] P. G. de Gennes, *Scaling Concepts in Polymer Physics* (Cornell University Press, Ithaca, NY, 1979).

[23] H. Kudo, K. Suga, and M. Fujihira, Chem. Lett. **36**, 298 (2007).
[24] B. Li, X. Fang, H. Luo, E. Petersen, Y. S. Seo, V. Samuilov, M. Rafailovich, J. Sokolov, D. Gersappe, and B. Chu, Electrophoresis **27**, 1312 (2006).
[25] M. Tokarz, B. Akerman, J. Olofsson, J. F. Joanny, P. Dommersnes, and O. Orwar, Proc. Natl. Acad. Sci. U.S.A. **102**, 9127 (2005).
[26] A. Balducci, C. C. Hsieh, and P. S. Doyle, Phys. Rev. Lett. **99**, 238102 (2007).
[27] P. J. Shrewsbury, S. J. Muller, and D. Liepmann, Biomed. Microdevices **3**, 225 (2001).
[28] O. Kedem and A. Katchalsky, Biochim. Biophys. Acta **27**, 229 (1958).
[29] J. N. Israelachvili, *Intermolecular and Surface Forces* (Academic Press, London, 1985).
[30] H. Tanaka, J. Chem. Phys. **105**, 10099 (1996).
[31] T. Kato, Science **295**, 2414 (2002).